Azimuth moveout transformation—some promising applications

Satinder Chopra, Dan Negut, and Samo Cilensek, Arcis Corporation

Often the offset and azimuth distributions for both land and marine 3D seismic surveys are irregular and poorly sampled. There are many reasons for this, ranging from practical considerations such as access to the survey area to the sometimes prohibitive economics of acquiring a well sample survey.

Modifying the azimuth and offset distributions using azmuth moveout (AMO) has proven effective at improving the offset azimuth distribution of 3D data sets. Although AMO originally was developed to address the shortcomings of marine acquisition, present potential applications include land seismic and wide-azimuth surveys.

Introduced by Biondi et al. (1998), azimuth moveout (AMO) is a partial prestack migration process which rotates the azimuth and modifies the offset distribution of 3D prestack data during processing, without the need for detailed a-priori assumptions about the velocity function or geology. The process was named "azimuth moveout" due to its ability to modify the azimuth of the data. AMO is a wave-equation-based regridding algorithm that applies the correct kinematic, phase and amplitude transformation, and handles dipping geological strata and variable velocity relatively accurately. These characteristics set AMO apart as a seismic interpolator from conventional techniques. It can also be used to reduce the size of 3D prestack data sets by coherently stacking traces with similar absolute offsets and azimuths. This paper discusses the effectiveness of AMO application on different 3D seismic volumes and demonstrates the advantages that accrue in doing so.

The AMO process

AMO is defined as an operator that transforms 3D prestack data with a given offset and azimuth to equivalent data with different offsets and azimuths. In other words, AMO can transform a trace recorded with a source and receiver positioned at x_{s1},y_{s1} and x_{r1},y_{r1} into a trace recorded with a source and receiver positioned at x_{s2},y_{s2} and x_{r2},y_{r2}. A process that is somewhat similar (but not the same) to this transformation is DMO, which transforms nonzero-offset data to zero-offset data. However, these zero-offset data cannot be properly imaged by prestack depth migration. AMO transforms prestack data into equivalent nonzero-offset data that can be used as input to prestack depth migration. So the AMO formulation is derived from DMO, by starting from the definition of DMO in the frequency-wavenumber domain (Hale, 1984), and the definition of its inverse (Ronen, 1987).

Next, the stationary-phase approximation of the AMO operator expressed in the frequency-wavenumber domain is evaluated. This yields a time-space representation of the AMO operator that can be applied as an integral operator. This time-space formulation of the AMO operator can now be applied to irregularly spaced data, with the obvious caveat that, for an accurate implementation, AMO must avoid aliasing the data and operator.

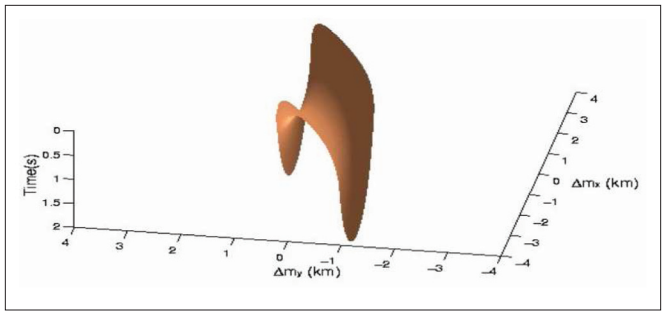

Figure 1. *Impulse response of a time-space AMO operator; it looks like a skewed saddle surface, with its width depending on the values of absolute offsets and azimuths.*

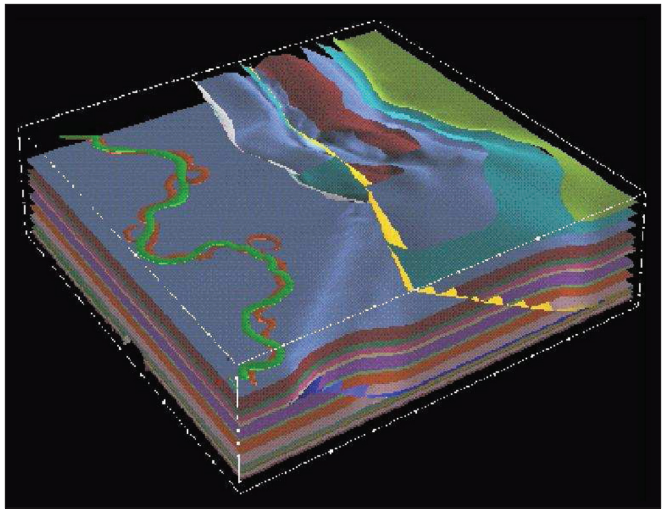

Figure 2. *Overthrust velocity model (cube view).*

Mathematically, AMO is conceived as a cascade of forward and reverse dip-moveout operators. The forward DMO transforms data from offset $\vec{h}_1$ to zero offset, and the reverse DMO transforms data from zero offset to offset $\vec{h}_2$. While DMO corrects for the true dip and also the shot-receiver azimuth effects on moveout velocity, AMO corrects for the azimuth effect only.

The impulse response of the time-space AMO is a skewed saddle surface (Figure 1); its width and dips depend on the values of absolute offsets and azimuths—i.e., the difference in azimuths between input and output data. The spatial extent of this saddle increases with the amount of azimuth rotation and offset continuation applied to the data. The AMO operator is compact and decreases in size with increasing time but, for small azimuth rotation and small offset continuation, the AMO operator is extremely compact and inexpensive to apply. Thus, the spatial extent of the operator is maximum for a rotation of 90° and vanishes for offsets and azimuths approaching zero. For more elaborate details about the process, the reader is referred to Biondi et al. (1998) and Biondi and Chemengui (2001).

AMO has many applications beyond its original use as a method to address the shortcomings of standard marine ac-

quisition. Matson and Abma (2005) have recently demonstrated an AMO based method to transform 2D SRME multiple predictions to 3D multiple predictions. We will describe how it can reduce prestack data volumes, interpolate land 3D seismic volumes, and regularize 3D land seismic volumes.

Reduction of prestack data

One important application of AMO is its ability to reduce the amount of 3D prestack data, without losing any information, by coherently stacking traces with similar azimuths and offsets. Since the kinematics of 3D data depend on azimuths and offsets, the data need to be processed with AMO before stacking, to maximize coherency among the traces that are averaged. This data reduction can make compute-intensive processes like 3D prestack time or depth migration, for example, more economical.

To illustrate the superiority of the AMO process, we tested it on the SEG/EAGE 3D overthrust model. We compared AMO followed by Kirchhoff migration with full Kirchhoff migration and with conventional binning followed with migration.

The overthrust model was designed to represent a realistic and complex geological situation (Figure 2). It depicts a complex, thrusted stratigraphy, unconformably overlying an earlier extensional and rift sequence topped with a complex weathering zone. The total model area is 20 × 20 × 4 km to allow realistic wide-azimuth seismic acquisition.

The stratigraphy and lithologies are those typical of an extensional zone of a mixed marine/terrigenous succession deposited upon evaporates. Channels and crevasse splay lenses are present in some layers. Velocities vary from 2178 m/s at the surface to 6000 m/s in the basement.

AMO was used to coherently stack the data along a reduced number of offsets and to a single azimuth, which reduced the data by more than a factor of 10. The reduced data set was subsequently imaged using 3D Kirchhoff prestack depth migration. Figure 3 shows a velocity slice through the 3D cube at y = 11,375 m. Figure 4 shows the result of the full 3D Kirchhoff depth migration at the same location. Figure 5, at the same location, is the result of Kirchhoff migration after AMO. Figure 6 shows the imaging after a factor-of-10 reduction. The input data were NMO-corrected, common-offset bins formed, data within an offset bin stacked, and inverse NMO applied using the offset at the bin center.

In comparing Figures 4 and 5, note that the image quality is very similar, although the latter was obtained ten times faster from the coherently reduced data set. The velocity model in this case is very complex, testing the AMO algorithm to its limit. However, in less complicated media, AMO followed by Kirchhoff migration is almost equivalent to full Kirchhoff migration.

In comparison with the standard NMO-bin-INMO result in Figure 6, AMO produces a much better quality image in such complex media. The weaker shallow fault on the right of the image is due to a strong mute used prior to NMO. The complex overthrust structure is correctly imaged, including the amplitude changes along the overthrust reflections due

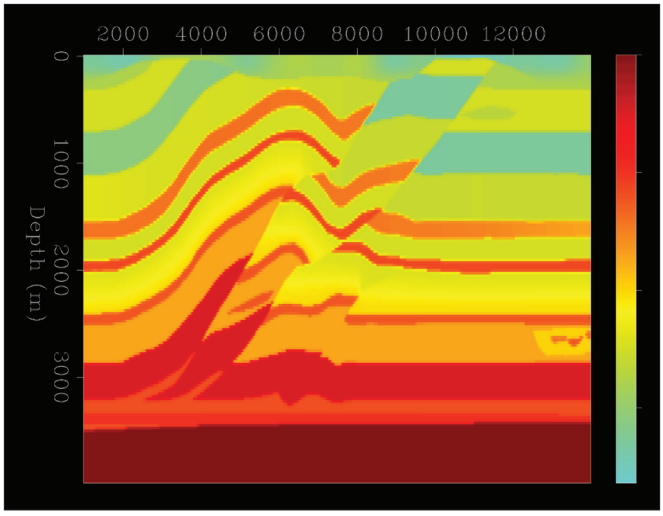

Figure 3. *Velocity (m/s) section through the SEG/EAGE overthrust data at y = 11,375 m.*

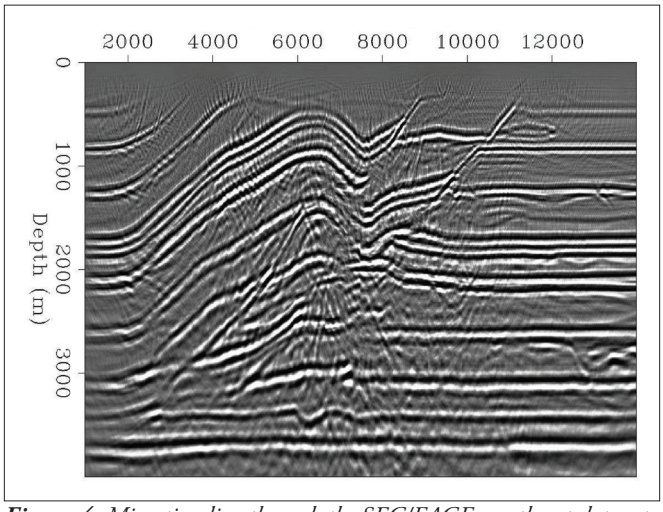

Figure 4. *Migration line through the SEG/EAGE overthrust data set after running 3D Kirchhoff depth migration (y = 11,375 m).*

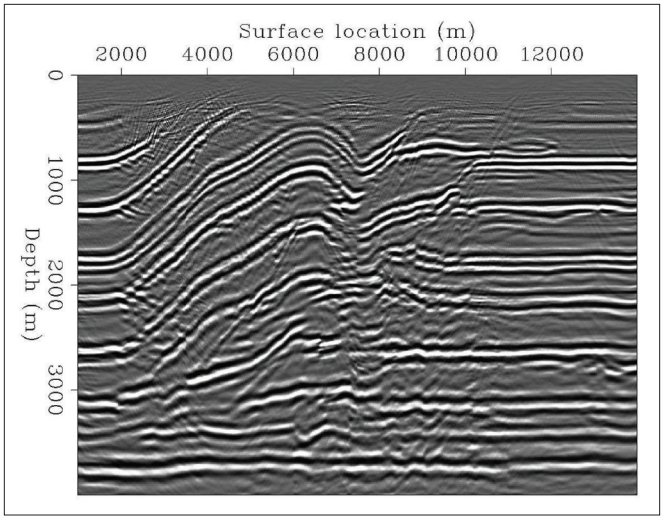

Figure 5. *Migration line through the SEG/EAGE overthrust data set after AMO (y = 11,375 m). The image accuracy of the AMO is very similar to the full Kirchhoff migration, although run at one-tenth of the cost.*

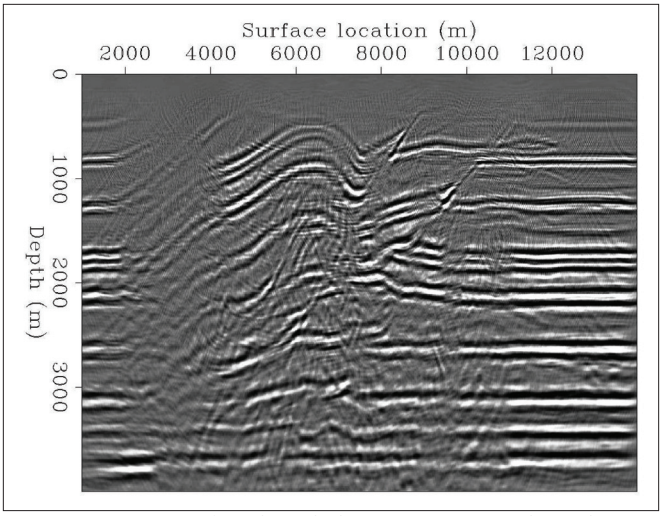

Figure 6. *Migration line through the SEG/EAGE overthrust data set after NMO, INMO, and Kirchhoff migration. This procedure produces a less accurate image.*

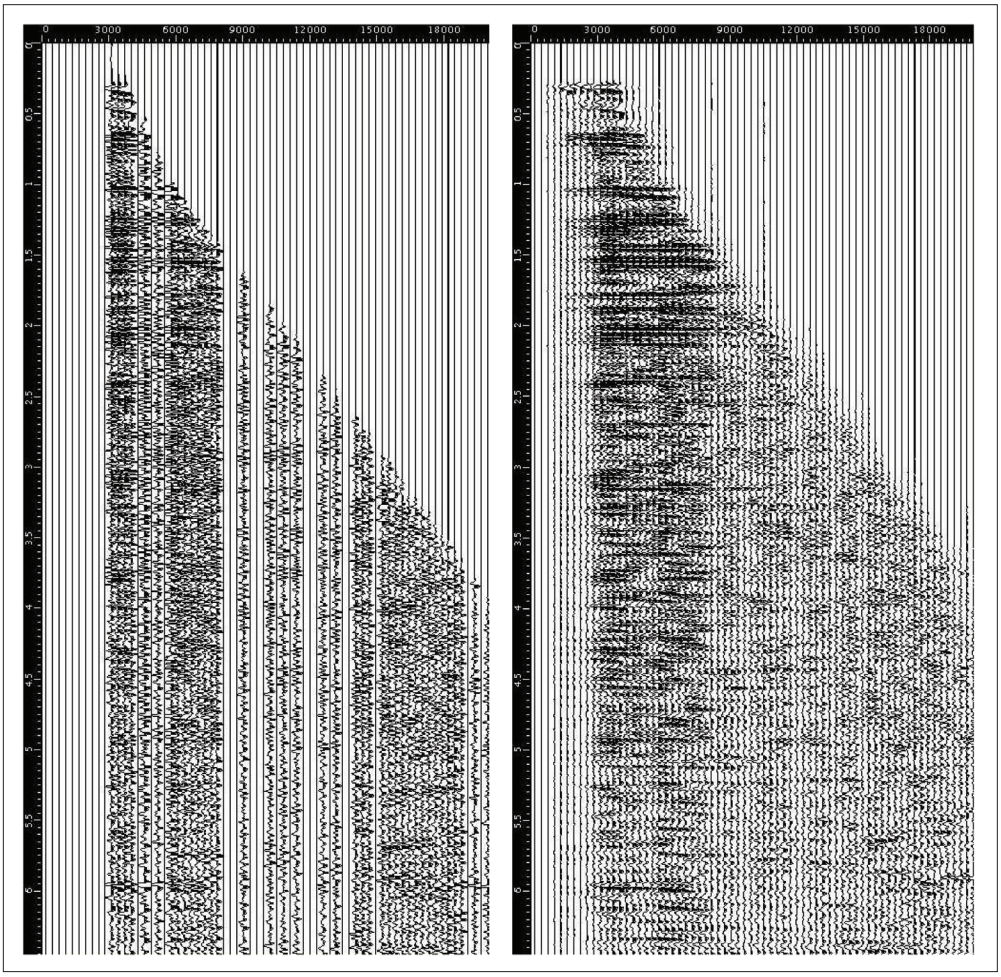

Figure 7. *Application of AMO for interpolation of missing offset (in feet) traces in a gather from a land data set. Left = before AMO. Right = after AMO. Note, on the AMO-processed gather, the improved signal-to-noise ratio and the coherency of the reflection events.*

to areas of changing impedance. The two main faults are correctly positioned, as are the main reflectors in the overthrust area, where major velocity changes occur.

Interpolation of 3D prestack data

AMO can be employed as a "wave-equation" interpolation of 3D data to overcome spatial aliasing problems or correct for uneven coverage.

Figure 7 is an example of the interpolation of data with AMO; it shows two gathers from a land data set where missing offsets are filled in during the wave-equation binning process. Notice how the AMO application improves the signal-to-noise ratio and the reflection events look more coherent and so can be easily interpreted.

Regularization of sparse and irregular geometries

Economic constraints and practical logistics during acquisition may cause the data to be sampled in a sparse or irregular fashion along one or more directions. For land data acquisition, physical obstructions and environmental objectives may prevent placement of source and receivers at the desired locations. Extra shots and receivers are also deployed at places that result in sparse coverage at some locations and an overabundance of traces at other locations. For marine data, cable feathering and swath or patch shooting can produce sparse or irregular distribution in offset, fold, or azimuth. Irregular sampling may also result from asymmetric shooting geometries and editing of noisy traces.

Various algorithms in the processing stream assume that the physical quantities such as time, source-receiver midpoint, azimuth, and offset are continuous. Kirchhoff migration is very sensitive to uneven sampling and can create strong amplitude distortions. Similarly, processes like DMO or algorithms employing any type of Fourier implementation require regular sampling. In reality and for the reasons mentioned above, one or more of these assumptions may not be true.

Wide-azimuth 3D surveys need an even range of source-to-receiver offsets at all azimuths and these need to be sampled adequately in space and time. However, in practice, offset and azimuth distribution could vary from bin-to-bin or could be uniform in say the inline direction and vary in the crossline direction. If not corrected properly, these irregularities can degrade

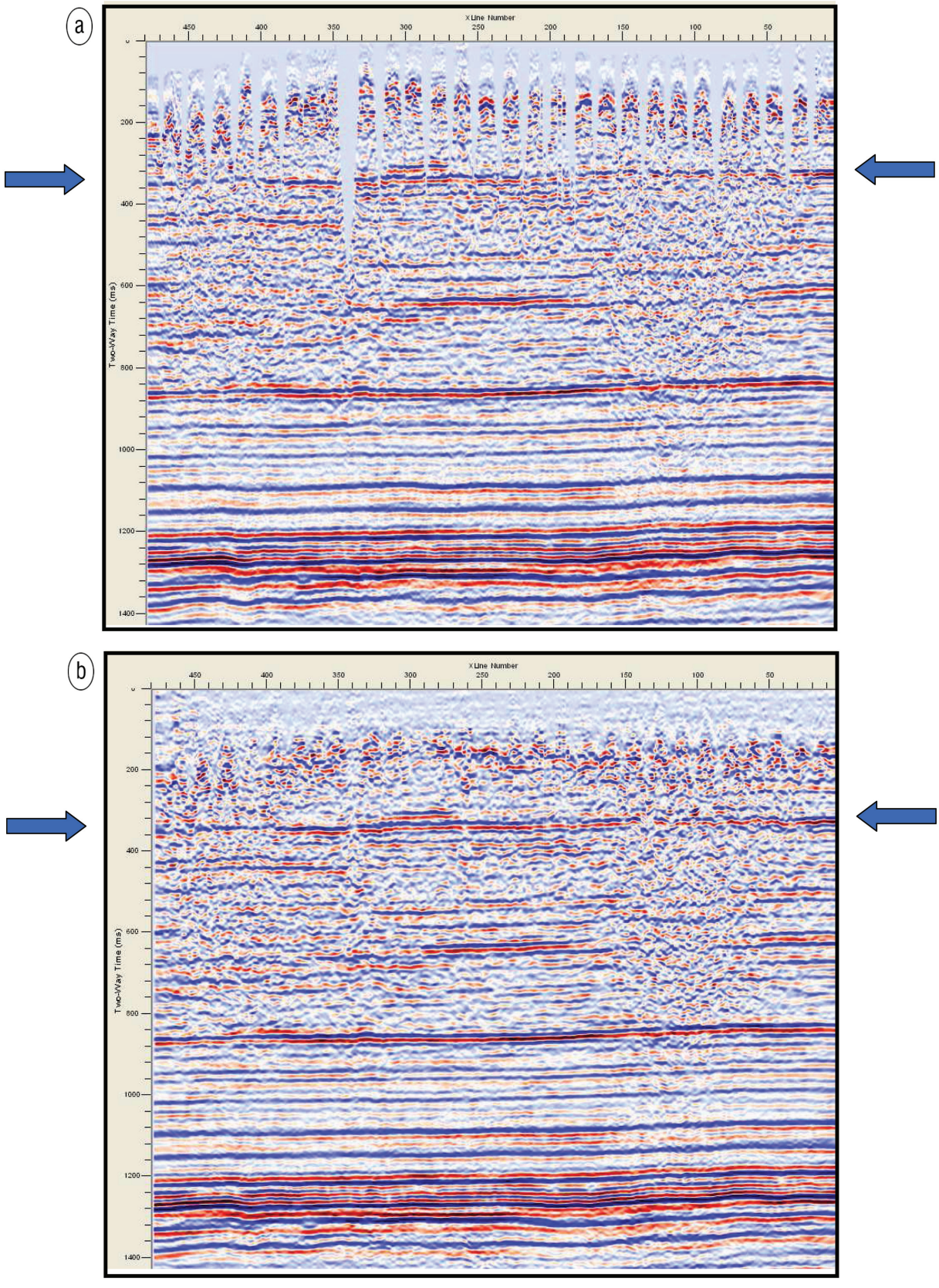

Figure 8. *An inline from a 3D seismic volume from central Alberta: (a) before and (b) after AMO application. Notice the data gaps at the shallow level before AMO application are filled up and the main reflection event (between the blue arrows) looks more focused and continuous.*

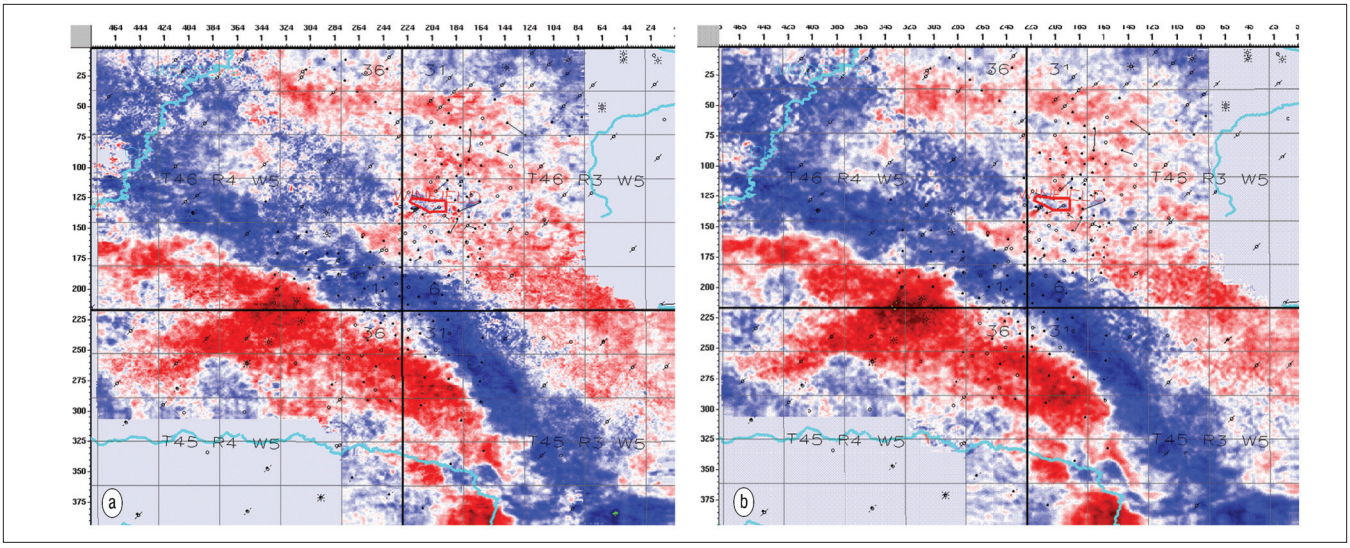

Figure 9. *Time slices at 850 ms from the same 3D seismic volume: (a) before and (b) after AMO application. AMO application results in more focused definition of the features.*

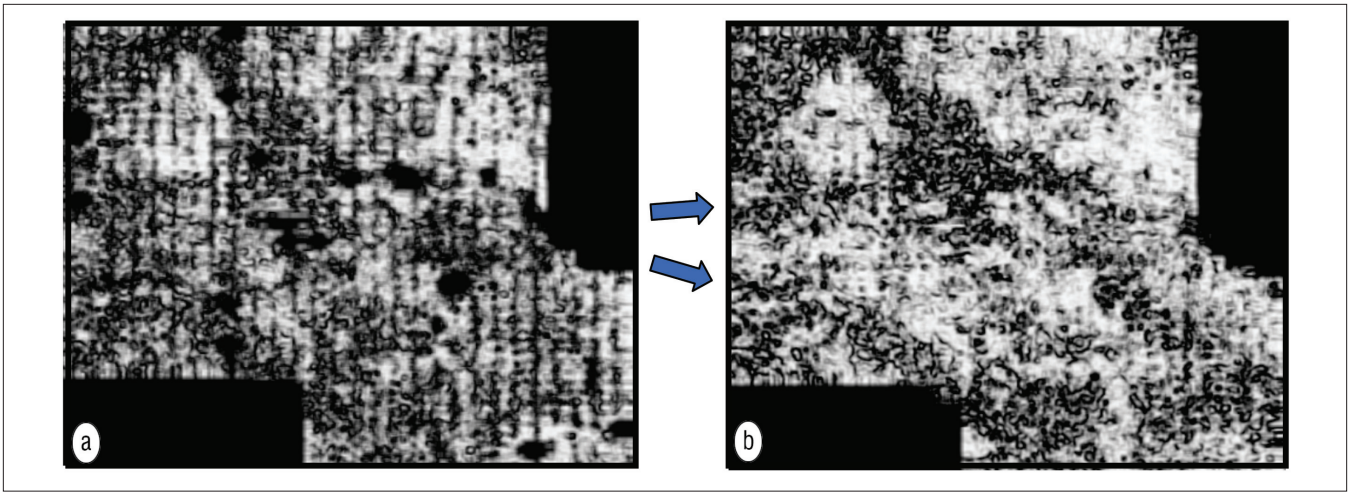

Figure 10. *Time slices at 320 ms from 3D coherence volumes: (a) before and (b) after AMO processing. The missing data gaps before AMO application are filled up after AMO processing, and at least two fault trends are seen clearly.*

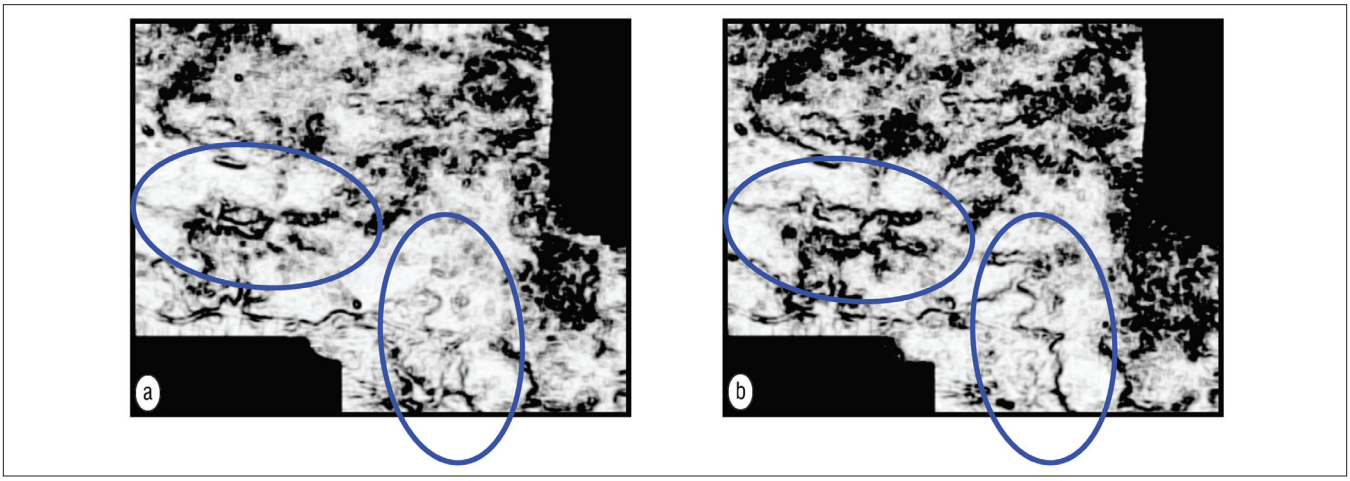

Figure 11. *Time slices at 1324 ms from 3D coherence volumes: (a) before and (b) after AMO processing. At this level, notice the distinct definition of the features in the highlighted zones, after AMO processing.*

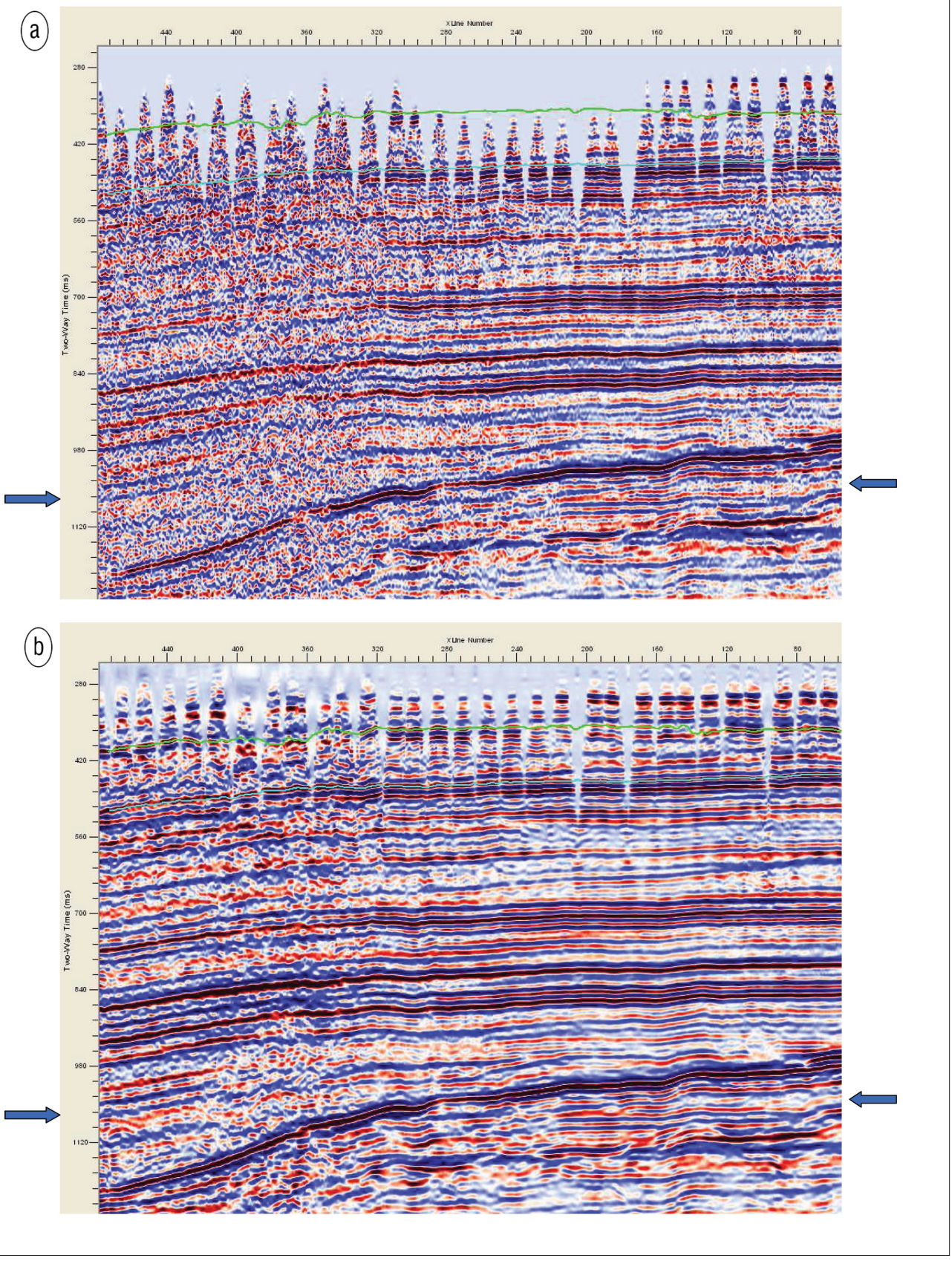

Figure 12. *An inline from a 3D seismic volume from Alberta: (a) before, and (b) after AMO application. Notice in (b) that the data gaps at the shallow level before AMO application are filled up, an appreciable improvement in the signal-to-noise ratio, and the main reflection events appear more focused and continuous.*

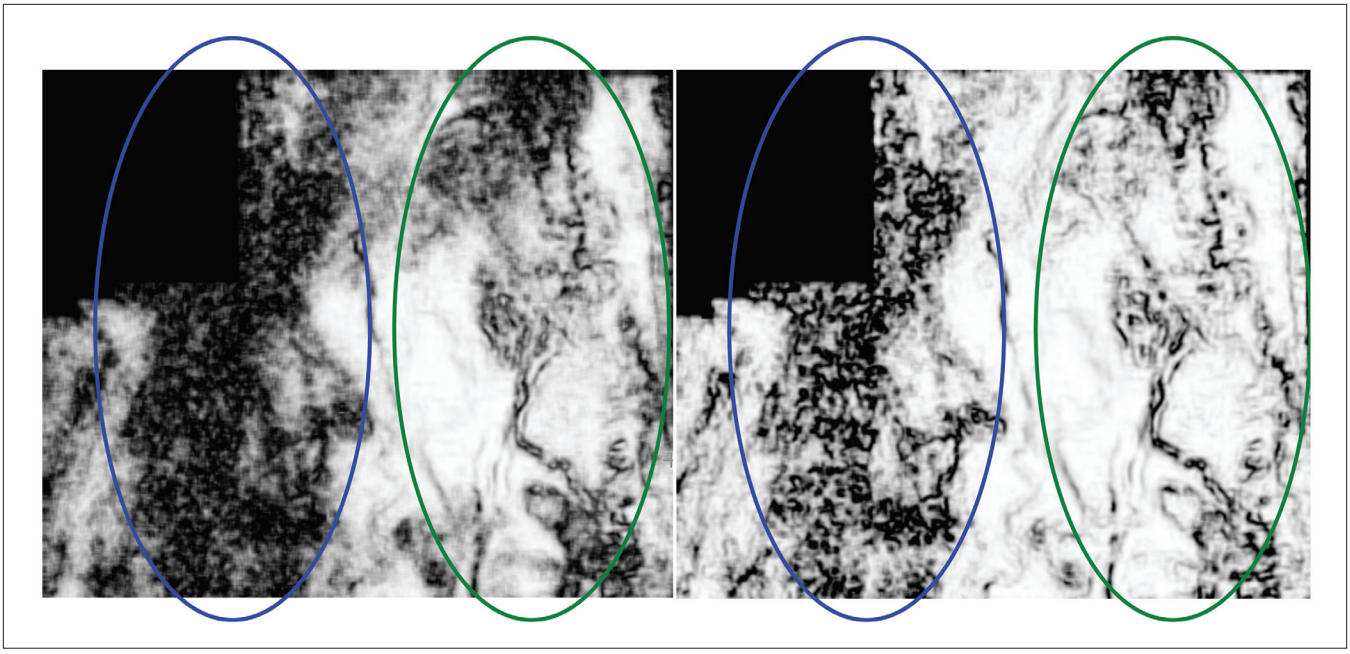

Figure 13. *Coherence time slices at 1018 ms from the same seismic volume in Figure 11. Left = before AMO. Right = after AMO. Because of the improved signal-to-noise ratio after AMO application, the coherence slice after AMO exhibits much better definition of the events (highlighted zones).*

stacks and cause amplitude artifacts and positioning errors in the final image, not to mention the fact that they can affect any prestack analysis that may be attempted. Neglecting azimuth variations results in incorrect computation of traveltimes which enter into various calculations during imaging. Conventional binning and interpolation techniques usually ignore the issue of source-receiver orientation and have the detrimental effect of averaging amplitudes over given areas.

Application of AMO can transform irregular 3D surveys with wide-azimuthal coverage onto regular midpoint-offset subsets with common source-receiver azimuths. After correction with AMO, the data have the necessary regularization and can be processed using any of the processes mentioned above as well as any of the wave-extrapolation methods including finite-differencing and wave-equation-domain techniques.

AMO was run on different 3D land data volumes and the effectiveness of the process was evaluated first by visual comparison of the seismic sections and time slices before and after AMO processing. This was followed by comparing coherence displays for AMO application, as it helps in assessing the differences better, due to its high spatial resolution.

Example 1

Figure 8a shows an inline before AMO from a land data set from central Alberta. Notice the gaps in the data in the shallow zone. Also, notice the discontinuous nature of the seismic reflection at approximately 360 ms (indicated with blue arrows). After AMO application (Figure 8b), the gaps are filled up and signal-to-noise ratio is also somewhat better. Notice how the main reflection at 360 ms now looks more continuous. The feeble reflections below the main event are also more focused and continuous. Figure 9 shows a pair of amplitude time slices from the seismic volume. Evidently, the AMO application makes the slice amplitudes more focused and sharp.

Figure 10 is a pair of coherence time slices (at 320 ms) from the same volume. Notice the areas of missing data along the receiver lines before AMO processing are filled up after its application. At least two fault trends can now be seen starting from the left, one running downwards and the other going to the right.

Figure 11 compares two coherence slices at 1324 ms from the same volume before and after AMO processing. In the highlighted zones, the events look sharper, suggesting that apart from the shallow levels, events at deeper levels also benefit from AMO application.

Example 2

Figure 12a and Figure 12b show a seismic inline from another 3D volume from Alberta, before and after AMO application. This example shows a pronounced improvement in the overall signal-to-noise ratio after AMO. Also, notice how the missing data gaps get filled up after AMO application and the reflections look more coherent and amenable for better interpretation. A set of coherence time slices at 1018 ms corroborates the above conclusions. The low coherence features to the left on Figure 13 appear less noisy. The definition of events in the highlighted zone appears to be much better after AMO application.

Another set of inlines from the same volume are shown in Figure 14. Again, better signal-to-noise ratio, filling missing data gaps, and more coherent reflections can be seen after AMO application. A pair of coherence horizon-slices at the level indicated (arrow) on the inlines in Figure 14, are shown in Figure 15. All events are now well defined and the interpretability of the data is definitely improved.

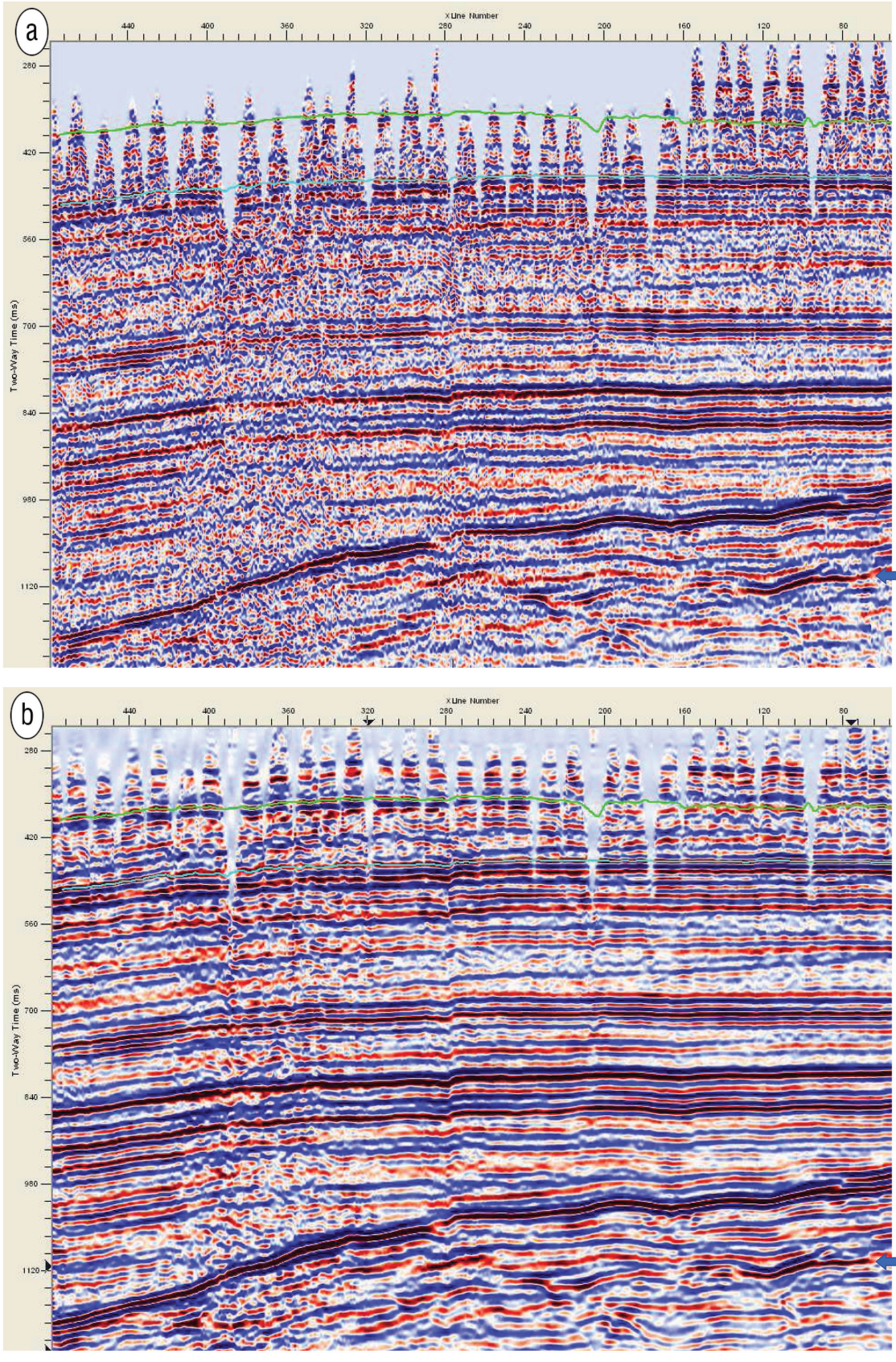

Figure 14. *An inline from the same 3D seismic volume: (a) before and (b) after AMO application. Notice in (b) that the data gaps at the shallow level before AMO application are filled up, appreciable improvement in the signal-to-noise ratio, and the main reflection events appear more focused and continuous.*

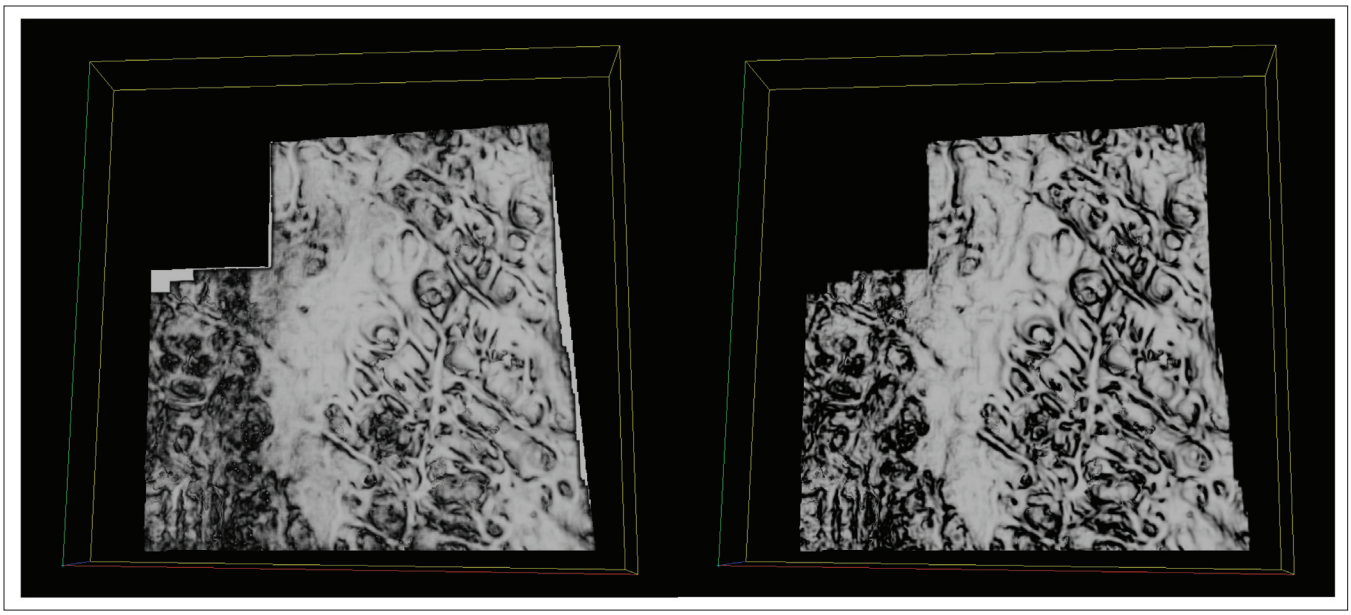

Figure 15. *Coherence strat-slices at the level indicated with arrows in Figure 14. Left = before AMO. Right = after AMO. Because of the improved signal-to-noise ratio after AMO application (Figures 11b and 13b), the coherence strat-slice in Figure 15b exhibits much better definition of the events.*

Conclusions

The effective offset and azimuth of 3D prestack data can be modified during the processing flow, with the application of AMO operator (partial migration operator) to the prestack data. The method addresses proper handling of irregular geometry and therefore allows reliable prestack analysis (AVO) analysis of migrated data. Improved signal-to-noise ratio and coherency of reflection events, and features showing up as crisp and distinct on time or horizon slices after AMO processing, enhance interpretability of poststack data.

Suggested reading. "Equalization of DMO for irregular spatial sampling" by Beasley et al. (SEG 1992 Expanded Abstrcts). "Azimuth moveout for 3D prestack imaging" by Biondi et al. (Geophysics, 1998). Transformation of 3D Prestack Data by Azimuth Moveout by Biondi and Chemingui (Stanford Exploration Project Report 80, 2001). "Amplitude preserving azimuth moveout" by Chemingui and Biondi (SEG 1995 Expanded Abstracts). "Handling azimuth variations in multistreamer marine surveys" by Chemingui and Baumstein (SEG 2000 Expanded Abstracts). "Dip-moveout by Fourier transform" by Hale (Geophysics, 1984). "Fast 3D surface-related multiple elimination using azimuth moveout for multiples" by Matson and Abma (SEG 2005 Expanded Abstracts). "Wave equation trace interpolation" by Ronen (Geophysics, 1987). TLE

Acknowledgments: The authors are grateful to Changjun Zhang, Sean Crawley, and Dimitri Bevc from our alliance partner company 3DGeo Inc., USA for providing the examples and for reviewing this paper and helping us with their useful comments. We also thank the personnel involved in AMO processing at Arcis Corporation, and to Arcis Corporation and 3D Geo Inc. for the support, permission to use the data examples, and permission to publish this paper.

Corresponding author: schopra@arcis.com